ACTA SIMULATIO

International Scientific Journal about Simulation

electronic journal
ISSN 1339-9640

2018 Volume 4 Issue 4

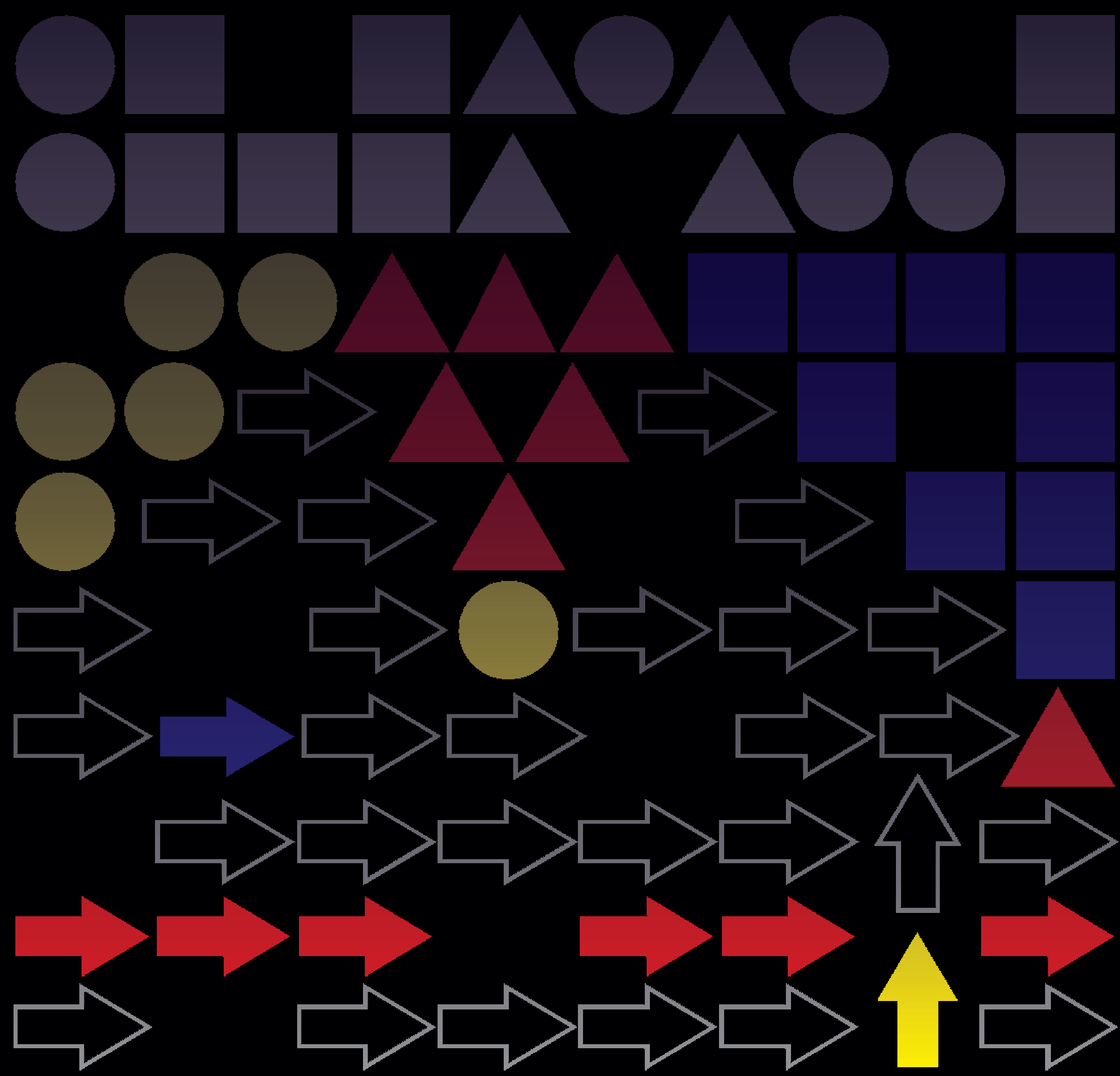

CONTENTS

(DECEMBER 2018)

Copyright © Acta Simulatio, www.actasimulatio.eu

Acta Simulatio - International Scientific Journal about Simulation
Volume: 4 2018 Issue: 4 Pages: 1-5 ISSN 1339-9640

doi:10.22306/asim.v4i4.54
Received: 29 Sep. 2018
Accepted: 07 Oct. 2018

3D LASER SCANNERS: HISTORY AND APPLICATIONS

Milan Edl
Faculty of Mechanical Engineering, University of West Bohemia in Pilsen, Univerzitní 22, 306 14 Plzeň, Czech Republic, EU, edl@fst.zcu.cz
Marek Mizerák
Technical University of Košice, Faculty of Mechanical Engineering, Institute of Management, Industrial and Digital engineering, Park Komenského 9, 042 00 Košice, Slovak Republic, EU, marekmizerak@gmail.com
Jozef Trojan
Technical University of Košice, Faculty of Mechanical Engineering, Institute of Management, Industrial and Digital engineering, Park Komenského 9, 042 00 Košice, Slovak Republic, EU, jozef.trojan@tuke.sk (corresponding author)

Keywords: 3D scanner, 3D scanning, laser, reverse engineering
Abstract: A 3D scanner is a device that analyzes a real-world object or environment to collect data on its shape and possibly its appearance (i.e. color). The collected data can then be used to construct digital three-dimensional models. 3D laser scanning developed during the last half of the 20th century in an attempt to accurately recreate the surfaces of various objects and places. The technology is especially helpful in fields of research and design. The first 3D scanning technology was created in the 1960s. The early scanners used lights, cameras and projectors to perform this task. Due to limitations of the equipment it often took a lot of time and effort to scan objects accurately. Collected 3D data is useful for a wide variety of applications. These devices are used extensively by the entertainment industry in the production of movies or virtual reality. Other common applications of this technology include industrial design, orthotics and prosthetics, reverse engineering and prototyping, quality control/inspection and documentation of cultural artifacts.

1 Introduction

In modern engineering, the term `laser scanning' is used to described two related, but separate meanings. The first, more general, meaning is the controlled deflection of laser beams, visible or invisible. Scanned laser beams are used in stereolithography machines, in rapid prototyping, in machines for material processing, in laser engraving machines, in ophtalmological laser systems for the treatment of presbyopia, in confocal microscopy, in laser printers, in laser shows, in Laser TV, and in barcode scanners.

The second, more specific, meaning is the controlled steering of laser beams followed by a distance measurement at every pointing direction. This method, often called 3D object scanning or 3D laser scanning, is used to rapidly capture shapes of objects, buildings, and landscapes.

Since the early 1980's, the analytical stereo-compiler has been the workhorse for broad-acre spatial data acquisition tasks including exploration mapping, regular mine planning and stockpile measurements (Byrne, 1997). It has also played a lesser role in subsidence monitoring, environmental lease statistics and infrastructure mapping.

Terrestrial laser scanning has already found its place between the standard technologies for objects acquisition. The laser scanner can be described as a motorized total station, which measures automatically all the points in its horizontal and vertical field. For each measured point, its distance to the laser scanner together with the horizontal and the vertical angles are recorded. So, the space coordinates relative to the scanner position can be easily computed.

Hand-held laser scanners create a 3D image through the triangulation mechanism described above: a laser dot or line is projected onto an object from a hand-held device and a sensor (typically a charge-coupled device or position sensitive device) measures the distance to the surface (Figure 1).

The purpose of a 3D scanner is usually to create a point cloud of geometric samples on the surface of the subject. These points can then be used to extrapolate the shape of the subject (a process called reconstruction). If color information is collected at each point, then the colors on the surface of the subject can also be determined [1].

This article is focusing in presenting a brief look on the 3D laser scanners. In addition, it gives a general presentation about the 3D laser scanners' history and applications.

Figure 1 3D lasser scanner Faro for industrial scanning

Copyright © Acta Simulatio, www.actasimulatio.eu

2 History of 3D scanners

3D laser scanning developed during the last half of the 20th century in an attempt to accurately recreate the surfaces of various objects and places. The technology is especially helpful in fields of research and design. The first 3D scanning technology was created in the 1960s.

The early scanners used lights, cameras and projectors to perform this task. Due to limitations of the equipment it often took a lot of time and effort to scan objects accurately. After 1985 they were replaced with scanners that could use white light, lasers and shadowing to capture a given surface. Next is a brief history of the 3D scanning development.

With the advent of computers, it was possible to build up a highly complex model, but the problem came with creating that model. Complex surfaces defied the tape measure as shown in figure 2.

Figure 2 Object tape measuring

By the mid-nineties they had developed into a full body scanner as shown in figure. This is where 3D Scanners appeared.

In 1994, 3D Scanners launched REPLICA - which allowed fast, highly accurate scanning of very detailed objects. REPLICA marked serious progress in laser stripe scanning.

Meanwhile Cyberware were developing their own high detail scanners, some of which were able to capture object colour too, but despite this progress, true three-dimensional scanning - with these degrees of speed and accuracy - remained elusive.

One company - Digibotics - did introduce a 4-axis machine, which could provide a fully 3D model from a single scan, but this was based on laser point - not laser stripe - and was thus slow. Neither did it have the six degrees of freedom necessary to cover the entire surface of an object, neither could it digitise color surface.

While these optical scanners were expensive, Immersion and Faro Technologies introduced lowcost manually operated digitisers. These could indeed produce complete models, but they were slow, particularly when the model was detailed. Again, they could not digitise color surface.

By this time, 3D modellers were united in their quest for a scanner, which was:

- accurate,
- fast,
- truly three dimensional,
-capable of capturing color surface,
- and realistically priced.

One of the first applications was capturing humans for the animation industry. Cyberware Laboratories of Los Angeles developed this field in the eighties with their Head Scanner as shown in figure (3).

Figure 3 Humans head scanning

In 1996, 3D Scanners took the key technologies of a manually operated arm and a stripe 3D scanner - and combined them in ModelMaker as shown in figure 3. This incredibly fast and flexible system is the world's first Reality Capture System.It produces complex models and it textures those models with color.

Color 3D models can now be produced in minutes. field in the eighties with their Head Scanner as shown in figure 4.

Figure 4 Manually operated arm and strip 3D scanner

3 3D laser scanning application

A virtual reality application may be employed to create a three dimensional virtual space from an existing architecture. The virtual reality space may then be used in computer simulations of various desired activities. Such activities could include a workflow or manufacturing line simulation [2].

The 3D virtual space may be used for entertainment, such as animation or a movie action scene simulation, keeping even the stunt professions safe from harm.

Copyright © Acta Simulatio, www.actasimulatio.eu

Transportation applications, such as a accident investigation. The scene of the accident could be 3D laser digitized, and a simulation of an actual accident event or "what if" scenarios explored.

3.1 Applications

3D laser scanning is used in a variety of fields and academic research. It has benefited clothing and product design, the automotive industry and medical science. Laser scanning can also be used to record buildings, especially in places that people may not be able to access due to safety hazards. 3D Laser Scanning is used in numerous applications: industrial, architectural, civil surveying, urban topography, mining, reverse engineering, quality, archaeology, dentistry, and mechanical dimensional inspection are just a few of the versatile applications. 3D laser scanning technology allows for high resolution and dramatically faster 3D digitizing over other conventional metrology technologies and techniques. Some very exciting applications are animation and virtual reality applications [3-5].

3.1.1 Material procesing and production

Laser scanning describes the general method to sample or scan a surface using laser technology. Several areas of application exist that mainly differ in the power of the lasers that are used, and in the results of the scanning process. Low laser power is used when the scanned surface does not have to be influenced, e.g. when it only has to be digitized. Confocal or 3D laser scanning are methods to get information about the scanned surface. Another low-power application are structured light projection systems that are used for solar cell flatness metrology enabling stress calculation with throughput in excess of 2000 wafers per hour.

3.1.2 Construction industry and civil engineering

- As-built drawings of Bridges, Industrial Plants, and Monuments.
- Documentation of historical sites.
- Site modeling and lay outing.
- Quality control.
- Quantity Surveys.
- Freeway Redesign.
- Establishing a benchmark of pre-existing shape/state in order to detect structural changes resulting from exposure to extreme loadings such as earthquake, vessel/truck impact, or fire.
- Create GIS (Geographic information system) maps and Geomatics.

3.1.3 Reverse engineering

Reverse Engineering refers to the ability to reproduce the shape of an existing object. It is based on creating a digitized version of objects or surfaces, which can later be turned into molds or dies. It is a very common procedure, which has diverse applications in various industries. Non-contact 3D laser scanning allows even malleable objects to be scanned in a matter of minutes without compression, which could change their dimensions or damage to their surfaces. Parts and models of all sizes and shapes can be quickly and accurately captured. 3D laser scanning for reverse engineering provides excellent accuracies and helps to get products to market quicker and with less development and engineering costs. 3D Laser scanning provides the fast, accurate, and automated way to acquire 3D digital data and a CAD model of part's geometry for reverse engineering when none is available. Also, new features and updates can be integrated into old parts once the modeling is accomplished [Site 12]. A practical mechanical and civil engineering application would be to assist in the production of "as built" data and documentation. Currently, many manufacturing or construction activities are documented after the actual assembly of a machine or civil project by a designer or engineering professional. 3D laser scanners could expedite this activity to reduce man-hours required to fully document an installation for legacy.

3.1.4 Mechanical applications

Reverse engineering of a mechanical component requires a precise digital model of the objects to be reproduced. Rather than a set of points a precise digital model can be represented by a polygon mesh, a set of flat or curved NURBS surfaces, or ideally for mechanical components, a CAD solid model. A 3D scanner can be used to digitize free-form or gradually changing shaped components as well as prismatic geometries whereas a coordinate measuring machine is usually used only to determine simple dimensions of a highly prismatic model. These data points are then processed to create a usable digital model, usually using specialized reverse engineering software [6-8].

3.1.5 Civil applications

Civil activities could be for a roadway periodic inspection. The digitized roadway data could be contrasted to previous roadway 3D scans to predict rate of deterioration. This data could be very helpful in estimating roadway repair or replacement costing information. When personnel accessibility and/or safety concerns prevent a standard survey, 3D laser scanning could provide an excellent alternative. 3D Laser scanning has been used to perform accurate and efficient as-built surveys and before- and after construction and leveling surveys [9].

3.1.6 Gargoyle models

The combined use of 3D scanning and 3D printing technologies allows the replication of real objects without the use of traditional plaster casting techniques, that in many cases can be too invasive for being performed on precious or delicate cultural heritage artifacts. In figure 5, the gargoyle model on the left was digitally acquired by using a 3D scanner and the produced 3D data was

Copyright © Acta Simulatio, www.actasimulatio.eu

processed using MeshLab software. The obtained digital 3D model was used by a rapid prototyping machine to create a real resin replica of original object as shown on the right of figure 5.

Figure 5 An example of real object replication by Means of 3D scanning and 3D printing

3.1.7 Medical CAD/CAM

3D scanners are used in order to capture the 3D shape of a patient in orthotics and dentistry. It gradually supplants tedious plaster cast. CAD/CAM (Computer-Aided Design/ ComputerAided Manufacturing) software are then used to design and manufacture the orthosis, prosthesis or dental implants.

Many Chairside dental CAD/CAM systems and Dental Laboratory CAD/CAM systems use 3D Scanner technologies to capture the 3D surface of a dental preparation (either in vivo or in vitro), in order to produce a restoration digitally using CAD software, and ultimately produce the final restoration using a CAM technology (such as a CNC milling machine, or 3D printer). The chairside systems are designed to facilitate the 3D scanning of a preparation in vivo and produce the restoration (such as a Crown, Onlay, Inlay or Veneer).

3.1.8 Design process

Design process including:

- Increasing accuracy working with complex parts and shapes,
- Coordinating product design using parts from multiple sources,
- Updating old CD scans with those from more current technology,
- Replacing missing or older parts,
- Creating cost savings by allowing as-built design services, for example in automotive manufacturing plants,
- "Bringing the plant to the engineers" with web shared scans, and
- Saving travel costs.

3.1.9 3D photography

3D scanners are evolving for the use of cameras to represent 3D objects in an accurate manner. Companies are emerging since 2010 that create 3D portraits of people (3D figurines or 3D selfies) (Figure 6) [10].

Figure 6 3D selfie

3.1.10 Law enforcement

3D laser scanning is used by the law enforcement agencies around the world. 3D Models are used for on-site documentation of:

- Crime scenes,
- Bullet trajectories,
- Bloodstain pattern analysis,
- Accident reconstruction,
- Bombings,
- Plane crashes, and more.

4 Conclusion

3D laser scanning equipment senses the shape of an object and collects data that defines the location of the object's outer surface. This distinct technology has found applications in many industries including discrete and process manufacturing, utilities, construction, archaeology, law enforcement, government, and entertainment. Laser scanning technology has matured and developed in the past two decades to become a leading surveying technology for the acquisition of spatial information. Wide varieties of instruments with various capabilities are now commercially available. The high-quality data produced by laser scanners are now used in many of surveying's specialty fields, including topographic, environmental, and industrial. These data include raw, processed, and edited dense point clouds; digital terrain and surface models; 3D city models; railroad and power line models; and 3D documentation of cultural and historical landmarks.

3D laser scanners have a wide rang of applications which applicable to very small object to a wide range areas.

Acknowledgement

This article was created by implementation of the grant project APVV-17-0258 Digital engineering elements application in innovation and optimization of production flows.

Copyright © Acta Simulatio, www.actasimulatio.eu

References

[1] GREGOR, M., MEDVECKÝ, Š., ŠTEFÁNIK A., FURMANN, R., MAČUŠ, P.: *3D laserové skenovanie veľkých objektov*, CEIT, Žilina, 2016. (Original in Slovak)

[2] BANGSOW, S.: *Manufacturing simulation with plant simulation and simtalk: Usage and programming with examples and solutions*, Springer Berlin, 2010.

[3] DRAHŇOVSKY, J.: *Maintenance organisation by the system TPM*, Proceedings of 6th International Doctoral Conference „JUNIORSTAV 2004“, Brno, VUT, p. 320, 2004.

[4] STRAKA, M: *Logistika distribúcie, Ako efektívne dostať výrobok na trh*, 1. ed., Bratislava, EPOS, p. 400, 2013. (Original in Slovak)

[5] GREGOR, M., MEDVECKÝ, Š., MIČIETA, B., MATUSZEK, J., HRČEKOVÁ, A.: *Digitálny podnik*, SCP, Žilina, 2006. (Original in Slovak)

[6] BUREŠ, M., ŠRAJER, V., GÖRNER, T.: *Projektování výrobních systémů a DP*, Ebook, SmartMotion, Plzeň, 2012. (Original in Czech)

[7] EDL, M., KUDRNA, J.: *Metody průmyslového inženýrství*, 1. ed., Plzeň: Smart Motion, s.r.o., 2013. (Original in Czech)

[8] FIĽO, M., MARKOVIČ, J., KLIMENT, M., TREBUŇA, P.: PLM systems and Tecnomatix Plant Simulation, a description of the environment, control elements, creation simulations and models, *American Journal of Mechanical Engineering*, Vol. 1, No. 7, p. 165-168, 2013.

[9] GÖRNER, T., ŠIMON, M.: *Případová studie ergonomického projektování pracovišť s využitím digitální továrny*, Digitálny podnik 2008, Žilina, Slovenské centrum produktivity, p. 99-104, 2008. (Original in Czech)

[10] Wikipedia: *3D scanning*, Online, Available: https://en.wikipedia.org/wiki/3D_scanning#cite_note-17, 2018.

Review process

Single-blind peer review process.

Copyright © Acta Simulatio, www.actasimulatio.eu

Acta Simulatio – International Scientific Journal about Simulation
Volume: 4 2018 Issue: 4 Pages: 7-10 ISSN 1339-9640

doi:10.22306/asim.v4i4.55
Received: 20 Oct. 2018
Accepted: 29 Oct. 2018

EFFECT OF A SURFACE ROUGHNESS ON THE CRACK DRIVING FORCE OF PHYSICALLY SHORT STATIONARY CRACK – NUMERICAL SIMULATION

Michal Kráčalík
Untere Hauptstraße 48/5, 2424 Zurndorf, Austria, michal.kracalik@gmail.com

Keywords: surface roughness, crack, crack driving force, J-Integral, numerical simulation
Abstract: The surface roughness, residual stresses and microstructure are main parameters that cause surface crack initiation in theoretically porous free materials. Hence, the effect of the surface roughness on the crack driving force is investigated regarding physically short stationary cracks in this paper. FE simulations show that mechanically short stationary cracks have practically zero crack driving force and the orientation of the crack driving force will not support crack growth. The crack driving force follows the material deformation around the crack tip in the opposite direction as is the supposed crack extension.

1 Introduction

Real surfaces are never really flat. Chemical, electrochemical treatment and generally production technology affect surface roughness [1] [2] [3] [4]. Surface roughness influences crack initiation and fatigue life of various materials under various mechanical and thermal loading conditions [5] [6] [7] [8] [9] [10]. From the mechanical point of view, surface roughness acts generally as a stress concentrator and influences fatigue life [11] [12] [13] [14]. From the fracture mechanics point of view, physically short cracks (further denotes only as short cracks) are substantially larger than the scale of the local plastic deformation with characteristic microstructural dimension usually smaller (in lengths) than 1-2 mm and they grow faster than physically long cracks (further only as long cracks) [15] – the threshold value is smaller compared to long crack [15] [16] [17].

The effect of the surface roughness on short crack is investigated by means of FE simulation. The simple plane stress FE Model evaluates crack driving force for three crack lengths and arithmetic surface roughness Ra. The FE Model does not take into account any crack closure mechanisms (review can be found in [18]). However, crack closure mechanism is not present, if crack starts to grow from small processing or metallurgical defects in form of pre-existing crack-like defect [19]. Explicitly is assumed that long cracks are not influenced by surface roughness and they are not investigated in the paper; the crack is modelled as a stationary crack (no crack extension is simulated).

Crack driving force concept is introduced in Chapter 2. FE Model is described in Chapter 3, results are presented in Chapter 4 and discussed in Chapter 5.

2 Crack driving force

The J-Integral is a crack driving force concept valid for nonlinear (and linear) material behaviour subjected monotonic loading; is defined as a path independent line integral and equal to the energy release rate [16]:

$$J = \int_{\Gamma} \left(w dy - T_i \frac{\partial u_i}{\partial x} ds \right), \qquad (1)$$

where w is the strain energy density, T_i is the traction vector (component), u_i is the displacement vector (component) and ds is length increment on the contour Γ.

3 FE Model

The FE plane stress model has a size of 100x100x10 µm. Mesh element size 1 µm is used in the whole model. The fix boundary conditions are prescribed in the bottom points in the FE model, see Figure 1. The Force F with magnitude 0.01 N is prescribed to the points in upper part of the Model. Scheme of the FE model is shown in Figure 1.

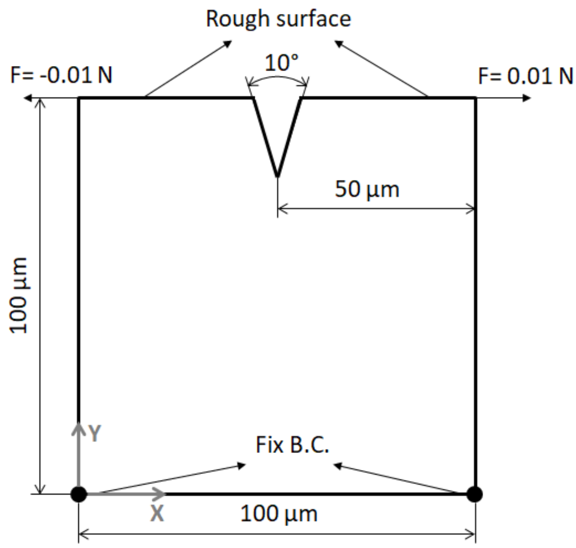

Figure 1 Scheme of the FE Model

Copyright © Acta Simulatio, www.actasimulatio.eu

Acta Simulatio - International Scientific Journal about Simulation
Volume: 4 2018 Issue: 4 Pages: 7-10 ISSN 1339-9640

One straight crack with length of 10, 20, 30 µm is embedded to the upper surface in the model. The crack has a wedge like geometry with opening angle of 10°. The crack is located either in the middle of the upper surface (X=50 µm) assuming a flat surface or approximately in the middle of the upper surface, see "Crack initiation" in Figure 2.

The arithmetic mean roughness Ra is modelled by the probability density function with the normal distribution in Python 3.6 (numpy library) with mean distribution of 3.2, 6.3 µm respectively; both with standard deviation 1 µm. The generated surface roughness is shown in Figure. 2. Generated points are imported to Ansys 16 and the rough surface is created.

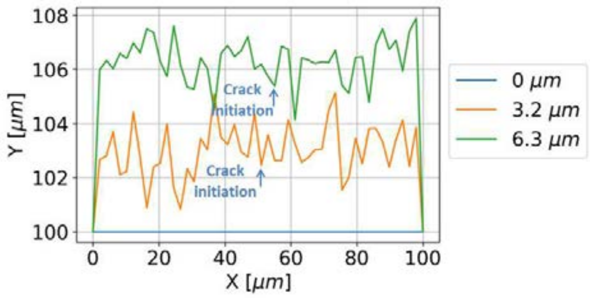

Figure 2 Arithmetic mean roughness Ra with marked crack initiation position. Crack initiation position is chosen approximately in the "roughness wedge" at the middle of the upper surface in order to reduce effect of the boundary condition in the FE model. Crack initiation on the flat surface (0 µm) is located at X position 50 µm.

A linear-elastic material model is used in the simulation with following parameters: Young's Modulus E=200 GPa, Poisson number ν=0.3. The local coordinate system of a crack is located at the crack tip. Mode I component (in the Y direction in global coordinate system) is evaluated.

4 Results

4.1 Numerical investigation

Figure 3 shows contour dependency of the computed crack driving force (J-Integral) for three crack lengths 10, 20, 30 µm. Flat surfaces is assumed in the simulations. Results show stabilization of the computed crack driving force since 3rd contour. Crack length of 10 µm demonstrates other trends of the computed crack driving force for 1st integration contour than crack lengths 20 and 30 µm, see Figure 3. The reason is irregular mesh for crack length of 10 µm created by automated mesh generation (soft meshing) in FE Software that influence results significantly; the mesh around other crack lengths is meshed regularly. Generally, it is not recommended usage of crack tip (1st integration contour) as a valid integration contour due to numerical accuracy [16]. The 3rd integration contour will be used in the further investigations.

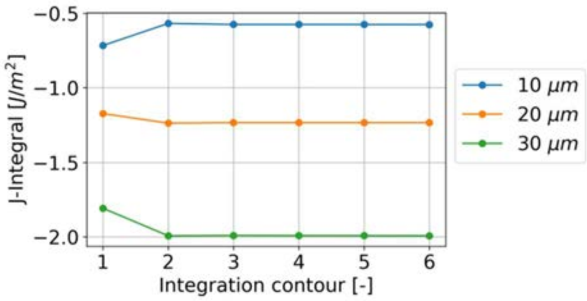

Figure 3 Contour dependency of the computed crack driving force (J-Integral) for three crack lengths (10, 20, 30 µm). Flat surface is assumed. 3rd and higher contour is numerically independent and will be used in further simulations.

The computed values are negative (related to the local coordinate system of a crack) - cracks have no tendency to growth. This phenomenon will be discussed in the next chapter.

4.2 Effect of the crack length and the surface roughness on the crack driving force

Figure 4 shows effect of the crack length and surface roughness on the crack driving force. Results for the 3rd integration contour are plotted. The longest crack (30 µm) has highest negative values – the crack has the smallest tendency to grow. The shortest crack (10 µm) has the "highest tendency to grow" – the values are in every investigated case negative. The material motion to the crack tip was observed in [20] but the context of the paper differs significantly from the presented one. The displacement field (material motion) will be discussed later in Chapter 4.3.

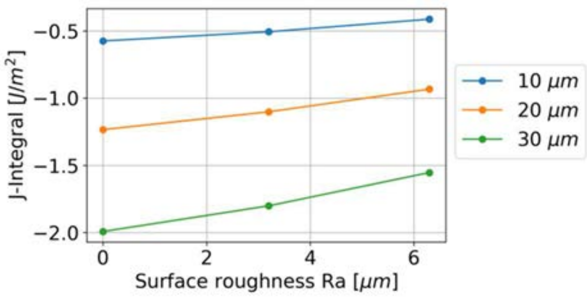

Figure 4 3rd integration contour of J-integral for three crack lengths (10, 20, 30 µm) over surface roughness Ra.

The surface roughness shifts negative values of crack driving force toward positive values but values are still negative (Figure 4). The computed results confirm observations that the crack propagation (and initiation) is supported by surface roughness [9] [12] [21] [22]. However, the continuum mechanics approach used in this paper has to be critically assessed regarding to short (stationary) crack, micromechanical approach and threshold values; more details can be found for instance in the review paper [23].

Copyright © Acta Simulatio, www.actasimulatio.eu

4.3 Displacement and stress field around the crack

Figure 5a shows displacement U_Y with marked non-deformed geometry and Figure 5b shows scoped perpendicular stresses on the crack S_{XX}. Scale 100 is used in Figure 5. The results are shown for crack length of 20 µm and Ra=3.2 µm.

The crack is moved in the up (Y) direction (a) and opened in crack Mode I (b). The maximum S_{XX} stresses are approximately 400 MPa around the crack tip (with prescribed force 0.01 N in the FE model).

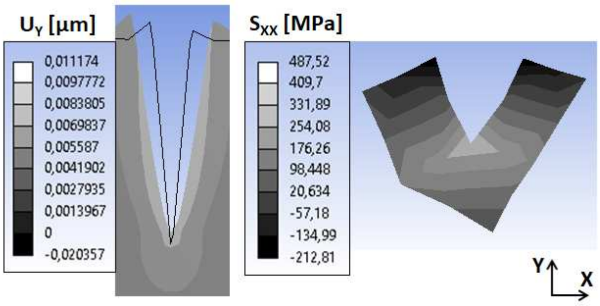

Figure 5 Displacement U_Y with marked non-deformed geometry (a). The crack is moved in the up (Y) direction. Scoped perpendicular stresses on the crack S_{XX} (b). The maximum stresses are approximately 400 MPa around the crack tip; the crack is opened – crack Mode I. The results are plotted for crack lengths of 20 µm and Ra=3.2 µm. The global coordinate system is used for plotting the result and scale 100 is used in the Figure.

The relationship between the J-integral and the displacement U_Y is plotted in Figure 6. U_Y is taken from the crack tip node. The deepest crack tip (30 µm) shows highest displacement upward and corresponding J-integral has the highest retardation tendency on the crack. Surface roughness decreases displacement upward and retardation effect on the crack decreases.

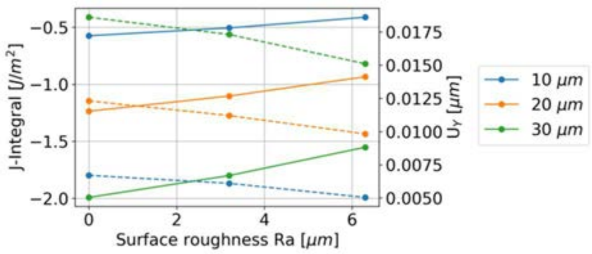

Figure 6 3rd integration contour of the J-integral (solid line) and the displacement U_Y (dashed line) for three crack lengths (10, 20, 30 µm) over surface roughness Ra. U_Y is taken from the crack tip node. The deepest crack tip (30 µm) shows highest displacement upwards and corresponding J-integral has the highest retardation tendency on the crack. Surface roughness decreases displacement upward and retardation effect on the crack decreases.

5 Discussion

The computed results are in accordance with two well observed phenomes. Firstly, the shortest crack (10 µm) would grow faster than longest cracks (20 and 30 µm) – the threshold value of small crack is smaller than longer cracks [15] [16] [17] [23] but clear distinction between microstructurally and physically small crack is not known. For instance, in [17] was for pearlitic steel chosen as the largest microstructural barrier 20 µm. This paper is focus only on physically short stationary cracks and the results should be assessed cautiously. Secondly, the high surface roughness leads to earlier crack initiation and smaller fatigue life than low surface roughness [9] [12] [21] [22] but this paper does not investigate crack initiation or fatigue life. Thus, the computed results are verified only indirectly.

Conclusions

The effect of a surface roughness on the crack driving force of stationary crack has been investigated in this paper. FE simulations show that crack driving force of physically short (stationary) crack follows material deformation and the surface roughness would support crack grow. This result is in accordance with experimental observations.

References

[1] KAJIKAWA, Y.: Roughness evolution during chemical vapor deposition, *Materials Chemistry and Physics*, Vol. 112, No. 2, pp. 311-318, 2008.
[2] BAEK, S.H., SHIM, H.-S., KIM, J.G., HUR, D.H.: Effect of chemical etching of fuel cladding surface on crud deposition behavior in simulated primary water of PWRs at 328 °C, *Annals of Nuclear Energy*, Vol. 116, No. June 2018, pp. 69-77, 2018.
[3] BONIN, L., CASTRO, C.C., VITRY, V., HANTSON A.-L., DELAUNOIS, F.: Optimization of electroless NiB deposition without stabilizer, based on surface roughness and plating rate, *Journal of Alloys and Compounds*, Vol. 767, No. October 2018, pp. 276-284, 2018.
[4] KRÁLIK, M., JERZ, V.: The Measurement of Residual Stresses in the Surface Layers of the Materials after Machining, *Materials Science Forum*, Vol. 919, No. April 2018, pp. 345-353, 5 2018.
[5] GALLO, P., BERTO, F.: Influence of surface roughness on high temperature fatigue strength and cracks initiation in 40CrMoV13.9 notched components, *Theoretical and Applied Fracture Mechanics*, Vol. 80, No. December 2015, pp. 226-234, 2015.
[6] LACERDA, J.C., MARTINS, G.D., SIGNORETTI, V.T., TEIXEIRA, R.L.P.: Evolution of the surface roughness of a low carbon steel subjected to fatigue, *International Journal of Fatigue*, Vol. 102, No. September 2017, pp. 143-148, 2017.

Copyright © Acta Simulatio, www.actasimulatio.eu

[7] WANG, J., ZHANG, Y., SUN, Q., LIU, S., SHI, B., LU, H.: Giga-fatigue life prediction of FV520B-I with surface roughness, *Materials & Design*, Vol. 89, No. January 2016, pp. 1028-1034, 2016.
[8] MOLAEI, R., FATEMI, A., PHAN, N.: Significance of hot isostatic pressing (HIP) on multiaxial deformation and fatigue behaviors of additive manufactured Ti-6Al-4V including build orientation and surface roughness effects, *International Journal of Fatigue*, Vol. 117, No. December 2018, pp. 352-370, 2018.
[9] BAGEHORN, S., WEHR, J., MAIER, H.J.: Application of mechanical surface finishing processes for roughness reduction and fatigue improvement of additively manufactured Ti-6Al-4V parts, *International Journal of Fatigue*, Vol. 102, No. September 2017, pp. 135-142, 2017.
[10] HAGHSHENAS, A., KHONSARI, M.M.: Damage accumulation and crack initiation detection based on the evolution of surface roughness parameters, *International Journal of Fatigue*, Vol. 107, No. February 2018, pp. 130-144, 2018.
[11] JAVIDI, A., RIEGER, U., EICHLSEDER, W.: The effect of machining on the surface integrity and fatigue life, *International Journal of Fatigue*, Vol. 30, No. 10-11, pp. 2050-2055, 2008.
[12] DAI, W.B., YUAN, L.X., LI, C.Y., HE, D., JIA, D.W., ZHANG, Y.M.: The effect of surface roughness of the substrate on fatigue life of coated aluminum alloy by micro-arc oxidation, *Journal of Alloys and Compounds*, Vol. 765, No. October 2018, pp. 1018-1025, 2018.
[13] SKALLERUD, S.K.ÅS,B., TVEITEN, B.W.: Surface roughness characterization for fatigue life predictions using finite element analysis, *International Journal of Fatigue*, Vol. 30, pp. 2200-2209, 2008.
[14] LIU, G., HUANG, C., ZOU, B., WANG, X., LIU, Z.: Surface integrity and fatigue performance of 17-4PH stainless steel after cutting operations, *Surface and Coatings Technology*, Vol. 307, No. December 2016, pp. 182-189, 2016.
[15] MAIERHOFER, J., PIPPAN, R., GÄNSER, H.-P.: Modified NASGRO equation for physically short cracks, *International Journal of Fatigue*, Vol. 59, No. February 2014, pp. 200-207, 2014.
[16] ANDERSON, T.L., ANDERSON, T.L.: *Fracture Mechanics: Fundamentals and Applications*, 3rd ed., CRC Press, 2005.
[17] KOLITSCH, S., GÄNSER, H.-P., PIPPAN, R.: Determination of crack initiation and crack growth stress-life curves by fracture mechanics experiments and statistical analysis, *Procedia Structural Integrity*, Vol. 2, pp. 3026-3039, 2016.
[18] PIPPAN, R., HOHENWARTER, A.: Fatigue crack closure: a review of the physical phenomena, *Fatigue & Fracture of Engineering Materials & Structures*, Vol. 40, No. 4, pp. 471-495, 2017.
[19] MAIERHOFER, J., KOLITSCH, S., PIPPAN, R., GÄNSER, H.-P., MADIA, M., ZERBST, U.: The cyclic R-curve – Determination, problems, limitations and application, *Engineering Fracture Mechanics*, Vol. 198, No. July 2018, pp. 45-64, 2018.
[20] FISCHLSCHWEIGER, M., ECKER, W., PIPPAN, R.: Verification of a continuum mechanical explanation of plasticity-induced crack closure under plain strain conditions by means of finite element analysis, *Engineering Fracture Mechanics*, Vol. 96, No. December 2012, pp. 762-765, 2012.
[21] WU, D., YAO, C., ZHANG, D.: Surface characterization and fatigue evaluation in GH4169 superalloy: Comparing results after finish turning; shot peening and surface polishing treatments, *International Journal of Fatigue*, Vol. 113, pp. 222-235, 2018.
[22] SHAHZAD, M., CHAUSSUMIER, M., CHIERAGATTI, R., MABRU, C., REZAI-ARIA, F.: Surface characterization and influence of anodizing process on fatigue life of Al 7050 alloy, *Materials & Design*, Vol. 32, pp. 3328-3335, 2011.
[23] ZERBST, U., VORMWALD, M., PIPPAN, R., GÄNSER, H.-P., SARRAZIN-BAUDOUX, C., MADIA, M.: About the fatigue crack propagation threshold of metals as a design criterion – A review, *Engineering Fracture Mechanics*, Vol. 153, pp. 190-243, 2016. 43, 2016.

Review process
Single-blind peer review process.

Copyright © Acta Simulatio, www.actasimulatio.eu

JOURNAL STATEMENT

Journal name:	**Acta Simulatio**
Abbreviated key title:	Acta Simul
Journal title initials:	AS
Journal doi:	10.22306/asim
ISSN:	1339-9640
Start year:	2015
The first publishing:	March 2015
Issue publishing:	Quarterly
Publishing form:	On-line electronic publishing
Availability of articles:	Open Access Journal
Journal license:	CC BY-NC
Publication ethics:	COPE, ELSEVIER Publishing Ethics
Plagiarism check:	Worldwide originality control system
Peer review process:	Single-blind review at least two reviewers
Language:	English
Journal e-mail:	**info@actasimulatio.eu**

The journal focuses mainly on the original and new, interesting, high-quality, theoretical, practical and application-oriented contributions to the field of science and research as well as to pedagogy and education in the area of simulation.

Publisher:	**4S go, s.r.o.**
Address:	Semsa 24, 044 21 Semsa, Slovak Republic, EU
Phone:	+421 948 366 110
Publisher e-mail:	**info@4sgo.eu**

Responsibility for the content of a manuscript rests upon the authors and not upon the editors or the publisher.